Using Atmospheric Polarization Patterns for Azimuth Sensing

Art Lompado*[a], Todd M. Aycock[a], Benjamin M. Wheeler[b]
[a] Polaris Sensor Technologies, 200 West Side Sq., Huntsville, AL, USA 35801[b]Naval Surface Warfare Center Dahlgren Division, 6096 Tisdale Rd., Dahlgren, VA, 22448

ABSTRACT

Unpolarized light from the Sun incident upon the Earth's atmosphere becomes polarized and presents a polarization pattern in the viewable sky dome that depends on the position of the Sun, the viewer's position on the Earth and the time of the observation. In clear and slightly overcast skies, both the degree of linear polarization and the polarization orientation can be predicted to first order using Rayleigh scattering theory. Conversely, measuring this polarization pattern provides information about the pose of a sensing platform equipped with an imaging polarimeter. We present here an investigation of the predicted polarization patterns in conjunction with a set of polarimetric measurements to show how the pointing direction of the platform hosting the polarimeter can be recovered. This direction derives solely from the measured polarization of a subsection of the hemispherical polarization pattern centered near the zenith and can be determined to high accuracy.

Keywords: Atmospheric polarization, polarimetry, polarimetric navigation, localization

1. INTRODUCTION

The phenomenon of scattering induced polarization has been well understood for many years and is the underlying mechanism by which unpolarized sunlight obtains a polarization signature upon interaction with the Earth's atmosphere. Polarization induced by scattering from atomic and molecular species within the atmosphere is well described using Rayleigh theory which requires that the scatterers be very small with respect to the incident wavelengths and that the scattered light undergoes a single scattering event prior to detection[1,2]. While these requirements can be restrictive, atmospheric scattering oftentimes satisfies them making the theory a powerful tool for predicting the observed polarization pattern across the visible hemisphere above the horizon. A polarimeter on the Earth's surface thus "sees" a polarization pattern across the viewable sky dome whose characteristics depend on the positions of the Sun, the sensor, and the target point in the sky. A full description of the polarization pattern of the clear sky requires a multiple scattering theory as provided by, for example, radiative transfer theory[3]. However, clear sky scattering is well approximated using Rayleigh theory and the resulting polarization pattern can be used to infer information about the sensor employed to measure this pattern. Our interest is in determining the pointing direction of a vehicular platform containing a polarimeter by using the measured polarization pattern to derive the platform's pose. Required information includes the sensor's position on the earth given in GPS coordinates and the measurement time which provides the position of the Sun. Coupled with the polarimeter's mounting configuration on the platform, the polarization at each point in the sky can be calculated. Inversely, a measurement of this polarization can be used to calculate the platform's pointing direction.

A number of investigators have reported on both the predicted[4,5] and measured[6,7,8,9,10,11] polarization patterns of both clear and overcast[12,13,14] skies. Still others have made inroads into the use of the pattern for navigation purposes[15,16,17,18]as is purportedly done by a host of biological creatures. We extend this body of work by presenting a practical application that uses the measured sky polarization pattern to accurately determine a platform's azimuthal pointing direction. For this work, the sensor was stationary and measurements of both clear and slightly overcast skies were acquired over an extended period. We show that despite the constantly changing polarization pattern, the stationary pointing direction is recovered to high accuracy and precision.

*Art.Lompado@PolarisSensor.com; phone 1 256 562-0087 x5667; fax 1 256 562-0088; PolarisSensor.com

2. POLARIZATION OF THE SKY – THEORY

The theory of polarization by scattering from a single nonabsorbing particle that is small compared to the incident wavelength was initially worked out by Rayleigh in the late 19th century. It represents a subset of Mie scattering and employs the small particle approximation to vastly simplify the requisite calculations for situations governed by the assumptions. Importantly, these restrictions can be satisfied by a scattering atmosphere due to both the small scatterer size and low scatterer density. This scattering occurs in the upper atmosphere and the assumptions break down when there is secondary and higher order scattering due to, for example, overcast skies or patchy clouds between the upper atmosphere and the sensor. According to the theory, the scattered light will be linearly polarized to varying degrees with a particular polarization orientation that depends on the geometry of the source-scatterer-sensor arrangement. The relevant polarization properties for navigation purposes include the degree of linear polarization (DoLP) and the angle of polarization (AoP) of the scattered light as viewed by the sensor. A single point polarimeter viewing a very small field of view (FOV) within the sky dome can measure the polarimetric response of that portion of the sky and, upon panning and tilting the sensor, a map of the sky polarization can be constructed. The DoLP of the measured position relates to the scattering angle θ, which is the angle between the light's initial direction connecting the Sun and target positions and the scattered light's new direction (i.e., from the target position to the sensor)The DoLP is given by[1]

$$\mathrm{DoLP} = \mathrm{DoLP}_{\max} \frac{1-\cos^2(\theta)}{1+\cos^2(\theta)} \tag{1}$$

where DoLP_{max} is the maximum detected DoLP and equals 1for an ideal(i.e., singly scattering) skyThe DoLP is a measure of the normalized magnitude of the polarization vector and ranges from 0 (unpolarized) to 1 (100% polarized) with intermediate values representing partially polarized light. Equation 1 can be derived based on the geometry of the source-scatterer-sensor arrangement and is useful for predicting the sky polarization properties but a second approach based on the Stokes vector can also be used and is more useful for measurements using a polarimeter. A linear polarimeter capable of measuring the first 3 elements of the Stokes vector (i.e., the linear components) can be used where the Stokes vector is given by[19]

$$\mathrm{SV} = \begin{pmatrix} S_0 \\ S_1 \\ S_2 \end{pmatrix} \tag{2}$$

Here S_1 represents the preference for horizontally polarized light over vertically polarized light, $S_1 = P_h - P_v$, while S_2 represent the preference for light polarized at 45° over light polarized at 135°, namely $S_2 = P_{45} - P_{135}$, where P_i is the power measured in polarization state i (i = h, v, 45, 135). The DoLP is related to the Stokes vector components through the following relationship

$$\mathrm{DoLP} = \frac{\sqrt{S_1^2 + S_2^2}}{S_0} \tag{3}$$

Thus, knowing the Sun, target, and sensor positions allows for prediction of the DoLP for any position in the sky using equation 1 while equation 3 allows for its calculation via polarimetric measurements. Typically, the Stokes vector employed is normalized meaning S_1 and S_2 range over [-1,1] and $S_0 = 1$. As expected, viewing the Sun directly, which implies no scattering, results in DoLP = 0 since θ = 0 and $S_1 = S_2 = 0$. Similarly, viewing a target position where θ = 90° (i.e., $S_1 = 1$, $S_2 = 0$) results in DoLP = 1. Employing Equation 1 at each possible pointing direction results in a predicted DoLP pattern on the visible hemisphere that can be represented with a polar plot obtained through the stereographic projection of the hemisphere down to a 2D surface. Figure 1 shows an example of this projection where the radial coordinate represents pointing altitude with the center being the zenith and the circumference representing positions along the horizon. The angular coordinate represents the viewing azimuth with the positive x and y axes representing North and East respectively. The Sun is shown as a yellow circle and the DoLP is seen to increase as one moves away from the Sun until it reaches a maximum wherever θ = 90°, after which it decays back to zero at the anti-Sun position.

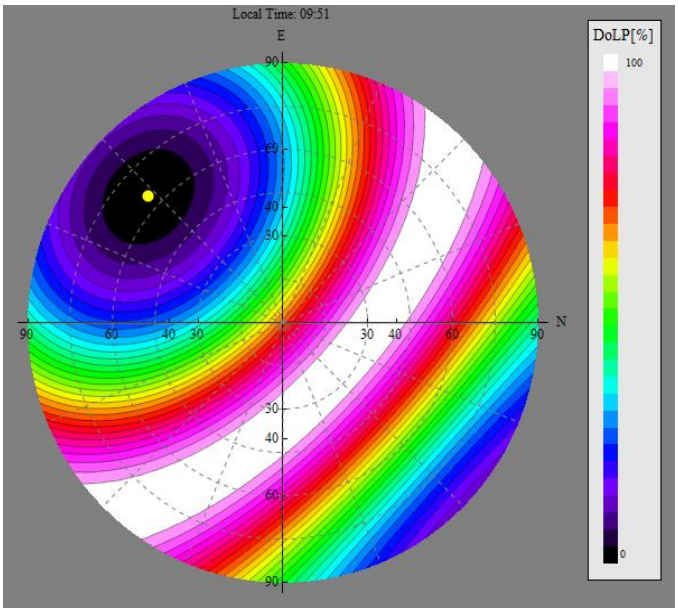

Figure 1. Stereographic projection of sky DoLP on 11-11-13 at 9:51 as measured from Huntsville, AL (Lat = 34° 43' 47.896", Long = -86° 35' 11.224").

The AoP is a measure of the polarization vector's orientation and ranges from 0° to 180°. It has been shown that the AoP points in a direction normal to the scattering plane which contains the Sun, target, and sensor. For any given time, sensor position, and target position in the sky, the AoP may be predicted based solely on the geometry of the situation. Additionally, Stokes vector measurements can be used to determine the AoP since[19]

$$\mathrm{AoP} = \frac{1}{2}\tan^{-1}\left(\frac{S_2}{S_1}\right) \tag{4}$$

Figure 2 shows the calculated AoP for the same viewing parameters as Figure 1. Again the Sun is shown by the yellow circle and a symmetric pattern is found with its axis of symmetry containing both the Sun and the zenith. For navigation

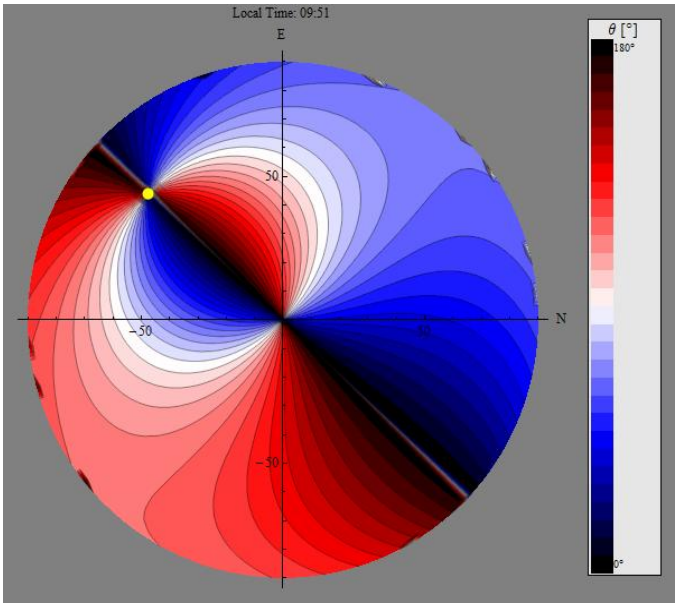

Figure 2. Stereographic projection of sky AoP on 11-11-13 at 9:51 as measured from Huntsville, AL (Lat = 34° 43' 47.896", Long = -86° 35' 11.224")

purposes, this map is more informative than the DoLP image of Figure 1 because a complete hemispherical image is not required to determine the Sun's position, which relates to the platform's pointing direction. Indeed the Sun itself need not be part of the predicted (or measured) region. Once enough data has been collected to identify the symmetry axis, the Sun's position can be inferred which in turn provides the platform's pointing direction since the sensor's location and the time of day are already known.

A shortcoming of the described approach is that it is based on a point sensor made to scan the available hemisphere to build up the images in the previous figures. Such scanning can be cumbersome and require enough time that the pattern can change over the course of the measurement. Instantaneous collection of the entire map is desirable and can be achieved through the use of an imaging polarimeter with a large FOV. Indeed, approaches using imaging polarimeters equipped with fisheye lenses have been reported and found to accurately match the predicted DoLP and AoP patterns. The advantages of such an approach go beyond simple snapshot imaging however because each pixel of the image shares a common coordinate system resulting in a different AoP map. In the case of a point imager, panning and tilting the sensor to different points in the sky causes rotations of the sensor's coordinate system which defines the AoP. An imaging polarimeter however assigns each position in the sky to a single pixel but all of those pixels share a single coordinate system. Mapping from a rotating coordinate system to a static coordinate system does not affect the DoLP map of Figure 1 since it is simply a magnitude measurement, but it does affect the AoP map. For an upward looking imager oriented so that its positive x and y axes point North and East respectively a transformation of coordinates maps Figure 2 into Figure 3 below. Note that Figure 3 has been plotted over the range [-90°, 90°] instead of [0°, 180°] to facilitate comparisons with measurements described below. The plot shows that there is a single contour line connecting the zenith and the Sun and implies that a measurement of AoP confined to the zenith region could be used to determine the angular position of the Sun, which in turn can be used to determine the platform orientation. This is important because it indicates that a limited FOV measurement can be used for navigation purposes so long as the zenith region of the sky remains relatively clear (i.e., single scattering prevails). A technique that employs measurements similar to Figure 3 but over a limited FOV has been used to prove the concept of sky polarization based navigation and is described in more detail below.

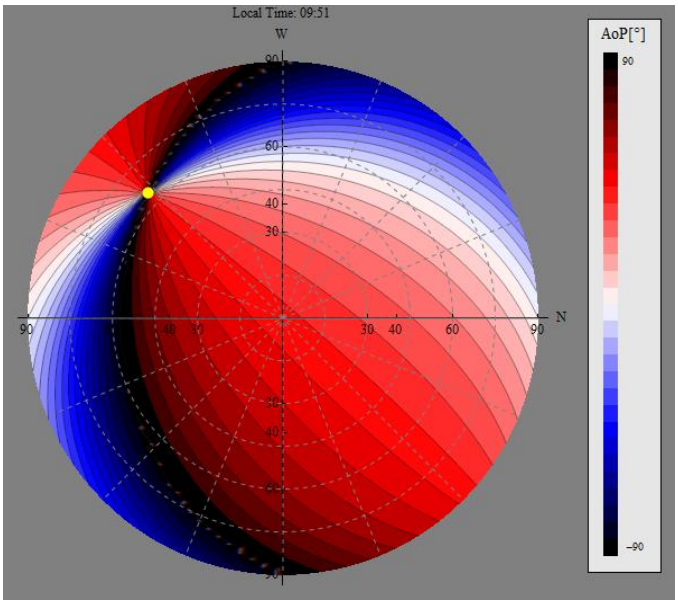

Figure 3. Stereographic projection of sky AoP for an imaging polarimeter. Acquisition parameters are the same as Figures 1 and 2.

3. POLARIZATION OF THE SKY – MEASUREMENTS

3.1 Polarimeter

Based on the theory of Section 2 a number of measurements were performed using an imaging polarimeter capable of measuring the first three Stokes vector components. The polarimeter has been described elsewhere [20] and employs the division of aperture architecture which is well suited for objects at infinity due to the essentially parallel chief rays in each quadrant. Figure 4 shows the back end of the polarimeter where the initial objective which creates an image at the labeled "intermediate object plane" has been omitted for clarity. The ray trace for only a single quadrant is shown for the same reason. Each quadrant, defined by one of four array lenses in a 2x2 configuration, creates an image of the target scene at its respective quadrant on the focal plane array (FPA). Three of the four polarimeter channels contain a uniquely oriented linear polarizer resulting in three uniquely polarized images in three of the four FPA quadrants. The sensor is polarimetrically calibrated prior to measurements using an integrating sphere and a calibration polarizer placed in front of the objective and made to rotate in 1° increments. The calibration procedure results in a data reduction matrix through which the three measured polarization images are mapped to determine the pixel resolved DoLP and AoP.

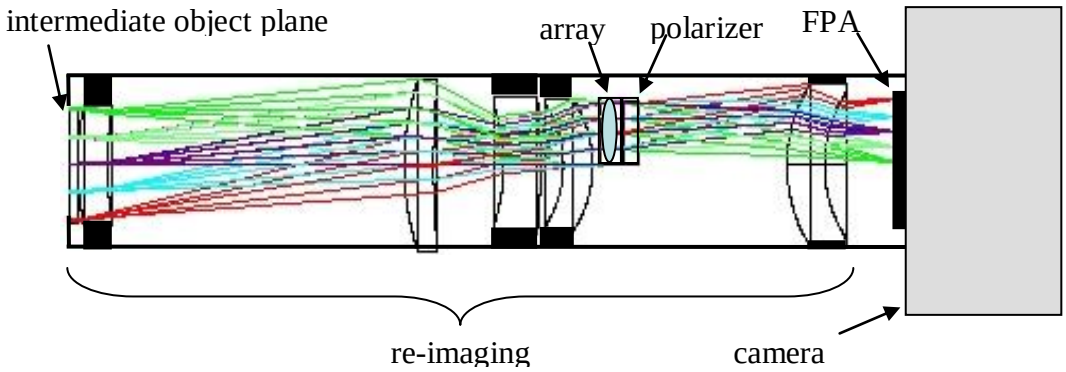

Figure 4. Schematic of imaging polarimeter showing ray trace of a single quadrant.

Some notes regarding the polarimeter are in order. First, the sensor was designed to image a 5° diagonal FOV but for this study it was operated using a 55.5° diagonal FOV (39.2° horizontal and vertical FOVs) obtained by reducing the objective's zoom factor. This change causes additional image distortion as described below. Second, the sensor's optic train contains a chipped lens which makes for a small anomaly on the imagery. Figure 5 shows an example of the raw image corresponding to the polarization resolved predictions of Figures 1-3 prior to the stereographic projection. The bright and dark spots in each subimage are due to the mentioned lens chip and dust respectively.

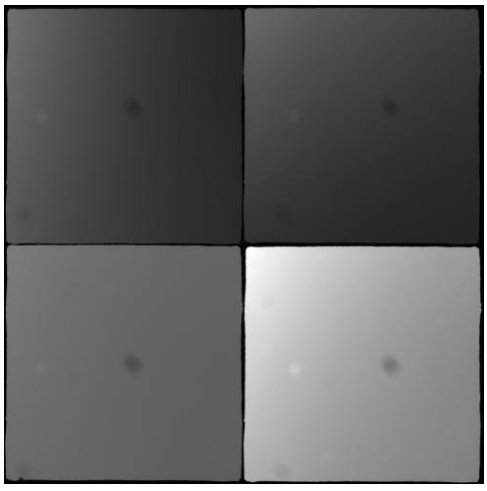

Figure 5. Raw polarimeter image showing four quadrant images. The lower right channel contains no polarizer and is thus brighter than the others.

3.2 Measurements

An experiment was performed to determine if the measured polarization of the sky dome could be used to derive the pointing direction of a platform hosting the polarimeter. The platform was a static tripod and measurements were performed over 6 (or more) hours in 1 minute intervals. The polarimeter was aligned by first pointing it to the West while its optical axis pointed horizontally. The westerly direction was obtained by placing the polarimeter outside and first measuring its GPS coordinates. Google Earth was then used to find a feature on the horizon that lied due west and the polarimeter was rotated to position that feature in the center of the quadrant images. The feature was a water tower located 2 miles from the polarimeter and consumed a single pixel in each subimage. Each subimage size was 512 x 512 pixels meaning the azimuthal positioning should be accurate to 39.2°/512 or 0.08°. The polarimeter was then tilted to point toward the zenith. Figure 6 contains three photographs including an image of the sensor in its horizontal position and one in its vertical operating position. The photograph in the lower left is taken across the top of the objective and shows the water tower feature used for alignment (red circle). Once oriented vertically, a digital level (accuracy = 0.1°) was used to pitch and roll the sensor to fine tune its pointing direction toward the zenith.

Figure 6. Photographs of the imaging polarimeter (top left), the polarimeter in operation (right), and a view across the objective at the water tower used for orienting the sensor (red circle).

Simulations of the expected DoLP and AoP based on the theory of Section 2 and the known sensor configuration and time were generated, and a region of angular size 39.2° x 39.2° centered at the zenith was extracted for comparison to the measurements. Careful alignment of the sensor precluded any secondary coordinate transformations so that a square region of angular extent 39.2° on a side and centered at the zenith of Figures 1 and 3 represents the expected measurement results. The sky was clear throughout the entire measurement duration. Figure 7 contains a comparison of the results for a single time, namely the first acquired image, with the top row showing the DoLP, the bottom showing the AoP, where the left and right columns contain the measured and predicted results respectively.

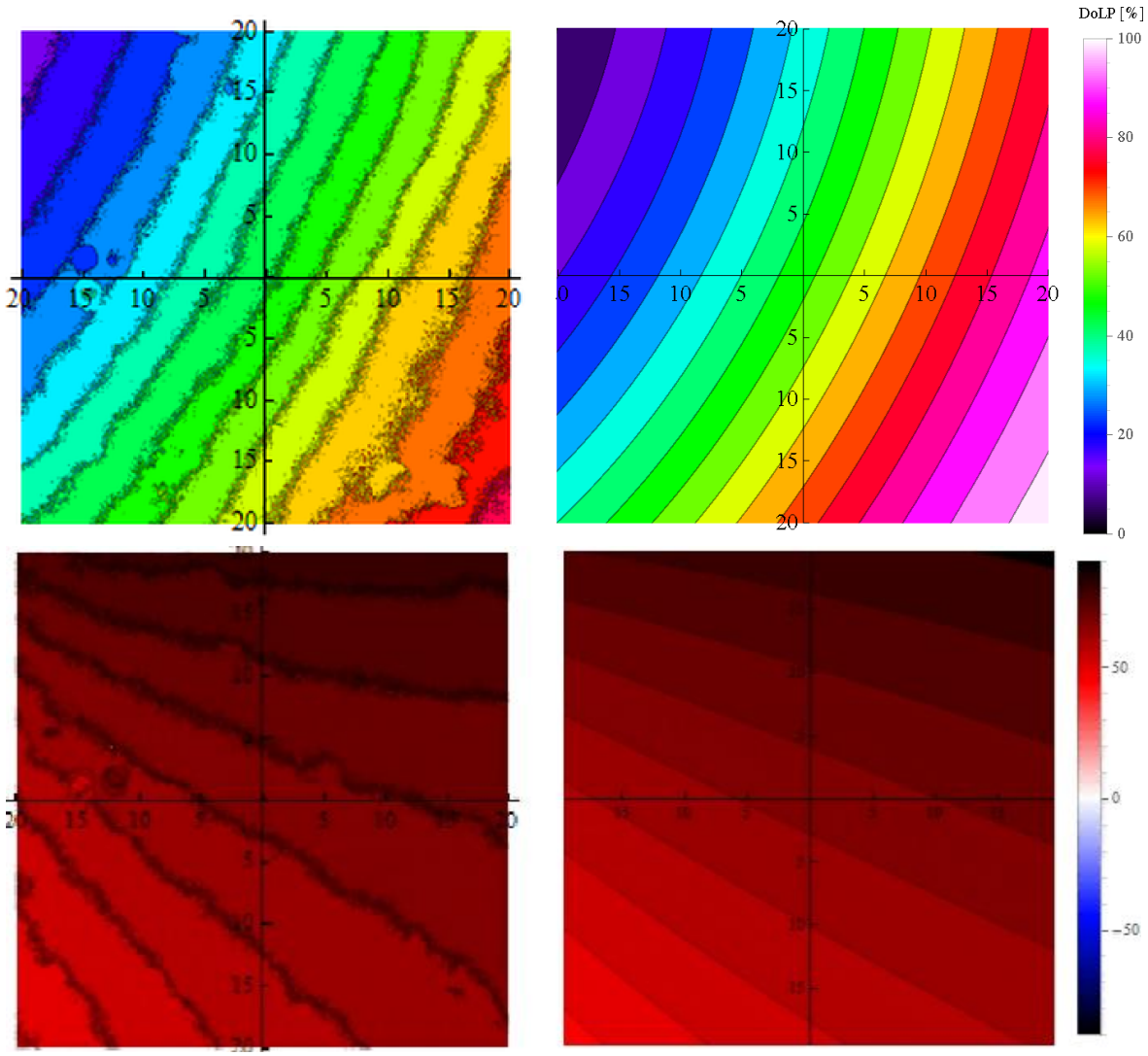

Figure 7. Comparison of measured and predicted DoLP (top) and the measured and predicted AoP (bottom) for a region 39.2° on a side and centered on the zenith. Axes values are degrees as measured from the zenith and the positive x and y directions represent the north and east directions. Scale bars indicate the magnitude of each plotted value.

The figures show very good correlation in both their shape and the magnitude of the plotted values excepting some minor discrepancies. The measured DoLP magnitude is lower than the predicted value since the assumption of single scattering is not completely satisfied, even in very clear skies. Also, both measured data products' contours do not exactly match the predictions due to the mentioned distortion in the imaging train of the polarimeter. Finally, the chipped lens artifact becomes more obvious in the reduced data although it only affects a small region near the x = -15° position. Nonetheless, the correlations are obvious despite these shortcomings and the measured results show potential for use in navigation applications. At this point there are a number of ways to analyze the data to obtain the platform's pointing direction. Recall the sensor in its horizontal position was pointed West, so we assign this as the pointing direction of the platform (i.e., the tripod). Considering only the AoP for now, Figure 3 indicated that a contour line exists connecting the Sun and the zenith so that a measurement of the AoP at the zenith is indicative of the Sun position. Since the sensor's GPS position and the time of the measurement are known, the azimuth of the Sun can be easily calculated and compared to the AoP at the zenith. Figure 8 contains a plot of the calculated Sun azimuth throughout the measurement and the measured AoP where the latter comes from an average of the measured values in a 1° FOV centered at the zenith. The curves are seen to have the same shape but differ in their measured angles by

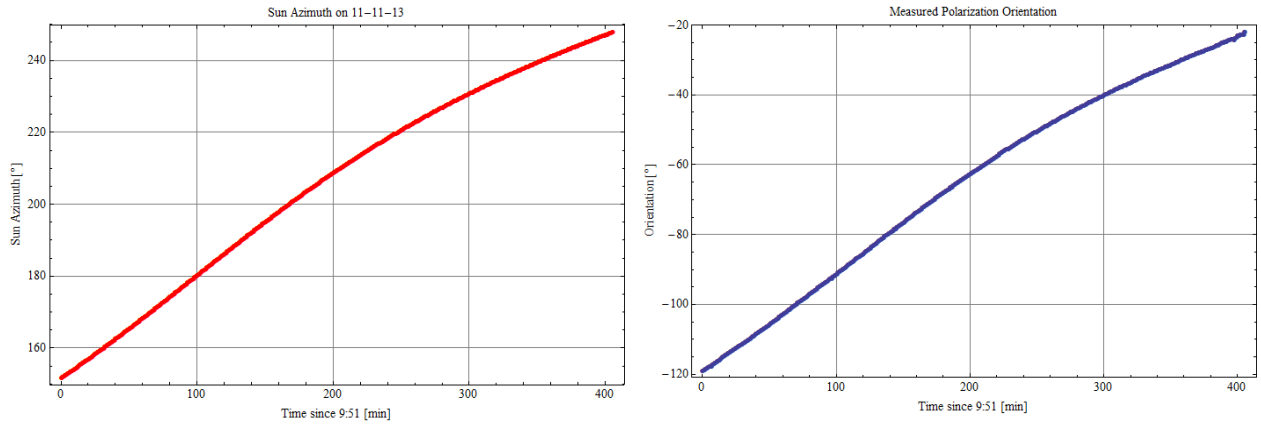

Figure 8. Left: Azimuth of the Sun during the measurement duration. Right: average of the measured AoP across a 1° FOV centered at the zenith

approximately 270°. Note that this difference represents the approximate platform pointing direction, i.e., West for a coordinate system where 0° represents North. A plot of the residuals between these data is shown in Figure 9 where the measured platform pointing direction is shown to be closer to 271° when examined across the entire measurement duration (271.0° ± 0.34°, mean ± SD). The ripple at the end of the plot is due to very low SNR during this time period as the Sun was descending below the horizon.

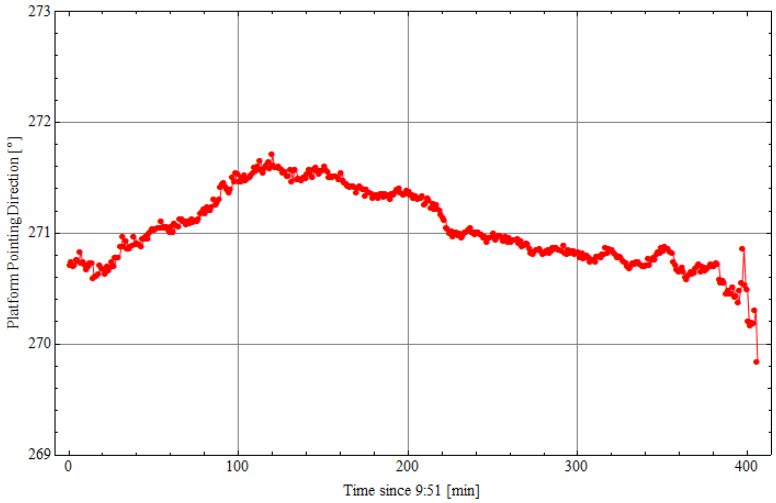

Figure 9. Platform pointing direction in 1 minute intervals obtained from the calculated Sun azimuth and the measured AoP over a duration of 6 hrs 50 min.

A second experiment was conducted on 11-04-13 during which the sky was at times clear, overcast, and thickly clouded. The purpose was to test the robustness of the approach in variable weather conditions. The experiment was conducted exactly as described for the 11-11-13 experiment. Note that using the measured orientation as the reference data product is a way of filtering the data since only light with a measurable polarization magnitude can have a defined orientation. That is, unpolarized light emerging from thick enough haze or clouds by definition has no orientation meaning any measurable orientation relates to the component of the light that transmitted through the haze/clouds unscathed. The measured orientation thus relates to the scattering atmosphere above the haze/clouds making for a way to continue to monitor the platform's pointing direction. Figure 10 contains both the calculated Sun position and the measured orientation after it has been shifted by 270°. The spikes and ripple seen in the AoP plot correspond to times when the haze/cloud cover was so thick that the orientation signature becomes unreliable (i.e., DoLP → 0).

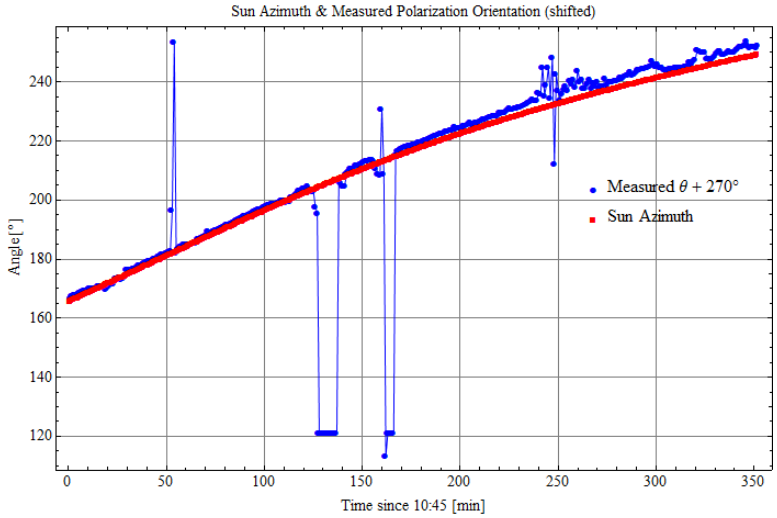

Figure 10. Sun azimuth (red) and measured AoP after being shifted by 270. Regions of large deviation between the plots represent times where haze/cloud cover were too thick to produce a reliable AoP measurement.

Figure 11 shows the same AoP plot as Figure 10 along with a sampling of three raw frames representing clear, clouded, and hazy conditions. Regions of the raw quadrants shown in red represent where the sensor has been soaked due to the additional scattering of the haze/clouds. The central image, where the zenith was obscured by a thick cloud, produces a spike in the measured AoP which obviously represents an unreliable data point. Importantly, although the last image was acquired in thick haze, it still produces a measurable AoP that can be used for navigation purposes.

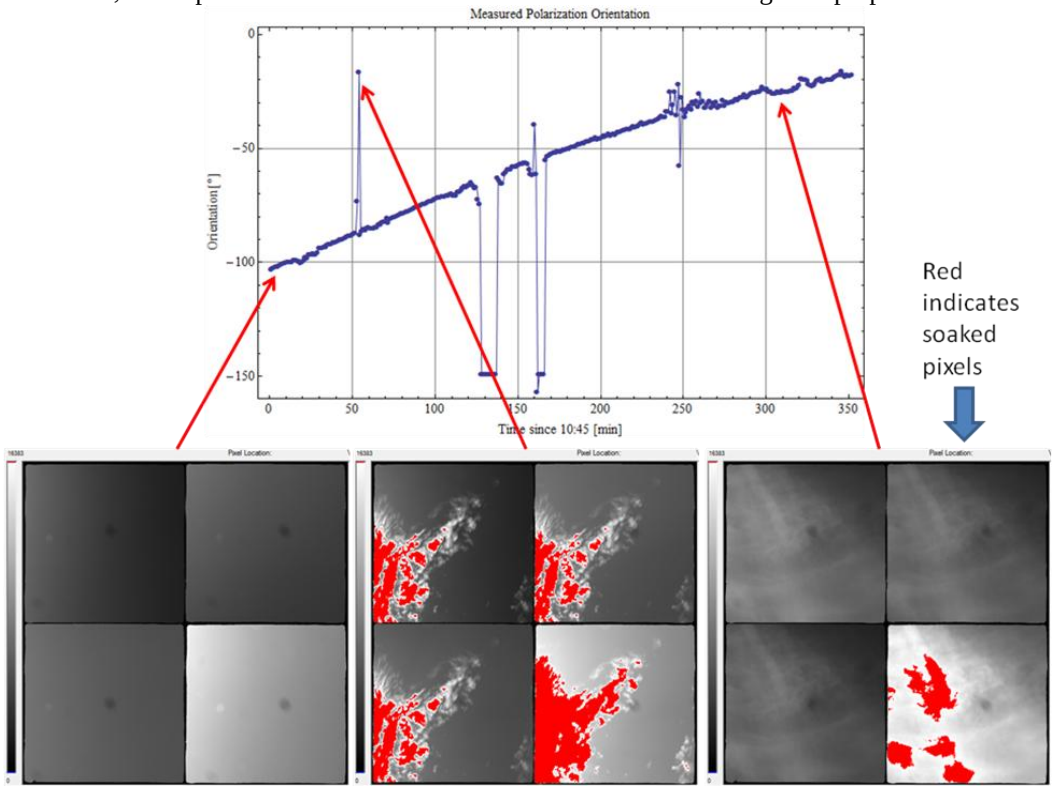

Figure 11. Measured AoP in varying haze/cloud cover. The bottom row shows the raw sensor images with soaked pixels are shown in red.Figure 12 shows the calculated platform pointing direction for the measurement of 11-04-13 and should be compared to Figure 9. Here, the presence of haze and clouds increases the overall variability in the calculated pointing direction, particularly in the case of heavy cloud cover as expected. Nonetheless, there are times where the presence of haze is

insufficient to render the pointing direction completely unreliable and the data is indicative of the pointing direction if not completely accurate.

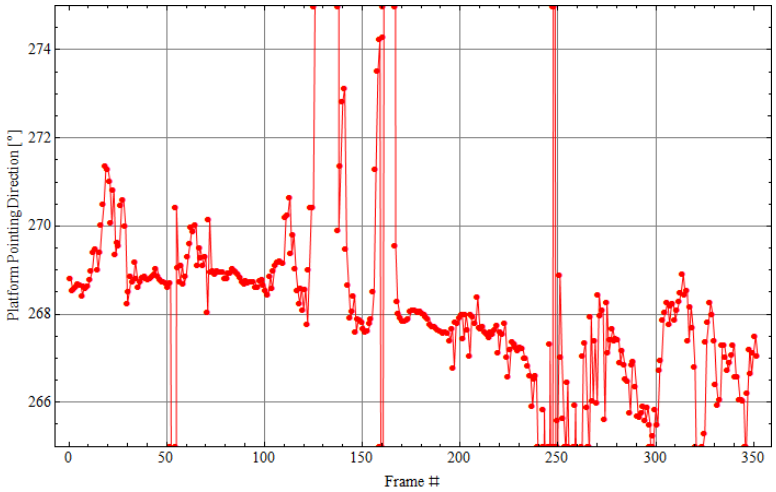

Figure 12. Platform pointing direction in 1 minute intervals obtained from the calculated Sun azimuth and the measured AoP during variable skies. Measurement duration was 5 hrs 52 min.

4. DISCUSSIONS AND CONCLUSIONS

The work described here makes obvious the potential of using sky polarization and, in particular, the measured AoP at the zenith for determination of the azimuthal pointing direction of a platform hosting a Stokes vector polarimeter. There is no need for imaging of the Sun and the technique can be used even in the presence of haze and cloud cover, albeit with reduced accuracy. Only a small subset of what can be gleaned from polarization imagery has been discussed and work continues to expand the capability. For example, filtering of the measured AoP using the measured DoLP represents a way to eliminate outliers that appear in the case of unclear sky measurements. Similarly, algorithms based on the measured intensity or the variation from frame to frame of intensity (or DoLP) can serve as filters to extract the reliable AoP data. Additionally, a conversion of the measured AoP in fixed FPA coordinates to AoP in rotating point sensor coordinates raises the potential of using the feature points unique to the latter map as a way to determine the pitch and roll of the platform hosting the polarimeter.

ACKNOWLEDGEMENTS

The authors gratefully acknowledge the support of the Office of Naval Research (Keith Hammack, and John Andrews) and the useful discussions with Terry Bollinger.

REFERENCES

[1] Bohren, C.F., and Huffman, D.R., [Absorption and Scattering of Light by Small Particles], John Wiley and Sons, Inc., New York, 130- 136, (1998).
[2] van de Hulst, H.C., [Light Scattering by Small Particles], Dover Publications, New York, Chap. 6 and 7, (1981).
[3] Chandrasekhar, S., [Radiative Transfer], Dover Publications, New York, 233-265, (1960).
[4] Smith, G.S., "The polarization of skylight: An example from nature," Am. J. Phys., 75(1), 25-35 (2007).
[5] O'Brien, D.M., "Numerical calculation of the transfer of polarized radiation by a scattering and absorbing atmosphere," CSIRO Atmospheric Research Technical Paper No. 49, 1- 66 (2001).
[6] Lee, R.L.,"Digital Imaging of clear-sky polarization," App. Opt., 37(9), 1465- 1476 (1998).
[7] Miyazaki, D., Ammar, M., Kawakami, R., and Ikeuchi, K., "Estimating sunlight polarization using a fish-eye lens," IPSP Journal, 49(4), 1234-1245 (2008).

[8] Gal J., Horvath, G., Meyer-Rochow, V.B., and Wehner, R, "Polarization patterns of the summer sky and its neutral points measured by full-sky imaging polarimetery in Finnish Lapland north of the Arctic Circle," Proc. R. Soc. Lond. A,, 457, 1385- 1399 (2001).
[9] Pust, N.J., and Shaw, J.A., "Digital all-sky polarization imaging of partly cloudy skies," App. Opt., 47(34), H190 – H198 (2008).
[10] Pust, N.J., Dahlberg, A.R., Thomas, M.J., and Shaw, J.A., "Comparison of full-sky polarization and radiance observations to radiative transfer simulations which employ AERONET products," Opt. Exp., 19(19), 18602- 18613 (2011).
[11] Dahlberg, A.R., Pust, N.J., and Shaw, J.A., "Effects of surface reflection on skylight polarization measurements at the Mauna Loa Observatory," Opt. Exp., 19(17), 16008- 16021 (2011).
[12] Pomozi, I., Horvath, G. and Wehner, R., "How the clear-sky angle of polarization pattern continues underneath clouds: full-sky measurements and implications for animal orientation," J. Exp. Biol., 204, 2933-2942 (2001).
[13] Hegedus, R., Akesson, S., and Horvath, G., "Polarization patterns of thick clouds: overcast skies have distribution of the angle of polarization similar to that of clear skies," J. Opt. Soc. Am. A, 24(8), 2347- 2356 (2007).
[14] Lee, R.L., and Samudio, O.R., "Spectral polarization of clear and hazy coastal skies," App. Opt., 51(31), 7499 – 7508 (2012).
[15] Guan, G., Gu, J., and Wu, M., "The Novel Method of North Finding Based on the Skylight Polarization," J. Eng. Sci. Tech. Rev., 6(1), 107-110 (2013).
[16] Sarkar, M., San Segundo Bello, D., van Hoof, C., and Theuwissen, A., "Biologically Inspired Autonomous Agent Navigation Using an Integrated Polarization Analyzing CMOS Image Sensor," Proc. Eng., 5, 673-676 (2010).
[17] Sarkar, M., San Segundo Bello, D., van Hoof, C., and Theuwissen, A., "Integrated Polarization Analyzing CMOS Image Sensor For Autonomous Navigation Using Polarized Light," 5th IEEE Int. Conf. on Intelligent Systems, 224-229 (2010).
[18] Karman, S.B., Diah, S.Z.M, and Gebeshuber, I.C., "Bio-Inspired Polarized Skylight Navigation Sensors: A Review," Sensors, 12, 14232-14261 (2012).
[19] Chipman, R.A., [Handbook of Optics, Vol II, 2nd Ed.], McGraw-Hill, Inc. New York, Chap 22, (1995).
[20] Moultrie, S., Roche, M., Lompado, A., and Chenault, D., "Design of a dual use imager incorporating polarimetric capabilities," Proc. SPIE 6682, (2007).